Mob-family kinase co-activators bind cognate Ndr/Lats kinases through conserved and modular interface

Benjamin Parker1, Gergő Gógl[2,3], Mónika Bálint[4], Csaba Hetényi[4], Attila Reményi[2] and Eric L. Weiss[1*]

[1]Northwestern University

[1,2] Lendület Protein Interaction Group, Institute of Enzymology, Research Center for Natural Sciences Hungarian Academy of Sciences, Magyar Tudósok körútja, 1117 Budapest, Hungary

[3]Department of Biochemistry, Eötvös Loránd University, Pázmány Péter sétány 1/C, 1117 Budapest, Hungary

[4]Department of Pharmacology and Pharmacotherapy, University of Pécs, Szigeti út 12, 7624 Pécs, Hungary

*To whom correspondence should be addressed: Eric L. Weiss: Department of Molecular Biosciences, Northwestern University, Evanston IL, 60208; elweiss@northwestern.edu; Tel. (847) 491-7034

Abstract

Ndr/Lats kinases bind to Mob coactivator proteins and their complexes play important roles in “Hippo” signaling pathways controlling cell proliferation and morphogenesis. All Ndr/Lats kinases have a 70-80 amino acid long unique N-terminal region (NTR) which binds to Mob factors. In order to gain insight into the structural basis of kinase-coactivator binding specificity, we have determined the crystal structure of Cbk1(NTR)-Mob2 and Dbf2(NTR)-Mob1 complexes from yeast (*S. cerevisiae*). We show that the Ndr/Lats(NTR)-Mob interface is a common structural platform through which kinase-cofactor binding is mediated, albeit amino acid variations in key positions contribute to subgroup and organism-specific differences. We further show that conserved residues at the NTR-Mob interface may participate in

novel activation mechanisms likely ubiquitous in Ndr/Lats kinases. Ndr/Lats kinase activation may resemble to that of other AGC kinases but with an extra structural requirement for NTR mediated Mob binding for proper allosteric activation.

Introduction

"Hippo" signaling systems are widespread in the eukaryotic world, playing roles in cell proliferation control, tissue development, and cell morphogenesis.[1] These pathways have a deeply conserved signaling core, in which Ste20-family Mst/*hippo* kinases phosphorylate a crucial activating site on an AGC-family Ndr/Lats kinase that binds a small, essential Mob coactivator protein. Activated Ndr/Lats – Mob complexes control cell processes by phosphorylating target effector proteins. In addition to demonstrating the broad preservation of this fundamental signaling axis, studies in *Drosophila*, budding and fission yeast, *C.elegans,* and other eukaryotes show that Ndr/Lats – Mob complexes control widely varying functional outputs (reviewed in[2–4]).

The Ndr/Lats kinases are divided into Ndr and Lats subfamilies with distinct amino acid sequences and cellular function .[3] In animals, for example, Lats-related kinases bind Mob1 and inhibit YAP/TAZ family transcriptional co-activators driving genes that promote cell cycle entry and apoptosis resistance; this system links cell proliferation to tissue organization.[1,2,5,6] Animal Ndr kinases associate with Mob2 coactivators, and play poorly understood roles in cell proliferation and morphogenesis of polarized structures.[1–4,6]. The Ndr and Lats subfamilies play distinct and well characterized roles in *S. cerevisiae* and *S. pombe*, distantly related fungal species. In *S. cerevisiae* the Lats-related kinase Dbf2 associates with Mob1 as central component of a system called the mitotic exit network (MEN) that controls the transition from M phase to G1[7–11] (reviewed in[12,13]) while the Ndr-subfamily kinase Cbk1 associates with Mob2 to control cell separation and polarized cell growth as part of a pathway called the RAM network.[14–21]. In the MEN the Mst/hippo-related kinase Cdc15 activates Dbf2; in the RAM

network the Mst/hippo related kinase Kic1 activates Cbk1. Notably, the overall architecture and functional output of the MEN and RAM network are largely similar in *S. pombe*.

Ndr/Lats kinases have a distinctive region immediately N-terminal to their kinase domains, referred to as the NTR (N-terminal regulatory) or SMA (S100B and Mob association); this is where the kinases' essential interaction with Mob-family coactivators occurs.[2,22,23] Discovered first in the *S.cerevisiae*, Mob1 is essential for cytokinesis and transit from mitosis to G1, and temperature sensitive Mob1 mutants arrest in telophase at restrictive conditions.[24–26] Mob1 binds Dbf2,[7,9,11,27,28] and *dbf2* mutants result in comparable phenotypes to that of *Mob1* alleles, such as cell-cycle arrest.[29,30] Mob2 functions similarly through the Cbk1 kinase.[14,19,20,31,32]

In *S.cerevisiae*, the cofactors Mob1 and Mob2 bind the Cbk1 (Ndr) and Dbf2 (Lats) kinases, yielding signaling complexes Dbf2-Mob1 and Cbk1-Mob2. Functionality of the cognates is constrained within confines of the RAM and MEN pathways, respectively, despite the simultaneous presence of both complexes in the cytosol (compare time courses observed in.[20,26,27,29] Indeed, the phosphatase Cdc14 is required for the function of Cbk1-Mob2 in the RAM network *in vivo*[20,33] and depends on the Dbf2-Mob1 complex for release from the nucleolus at the onset of mitotic exit.[34] Studies on homologous *Schizosaccharomyces pombe* Sid2(Lats)-Mob1 and Orb6 (Ndr)-Mob2 have further suggested fungal Ndr/Lats-Mob interactions are specific, with each Mob interacting with exactly one kinase,[35,36] despite the highly conserved nature of both the Mob cofactor and the kinase NTR across the family[2,37]. The similar *S.cerevisiae* Dbf2-Mob1 and Cbk1-Mob2 would not interchange their subunits within this paradigm. This insulation of cofactor binding distinguishes Ndr/Lats-Mob from the multifaceted interactions of cyclin-Cdk to which they have been compared.[9,38]

In contrast with budding yeast Mob1/2, humans have six Mob proteins (hMob1A/B, hMob2, hMob3A/B/C), of which hMob1A/B and hMob2 have been shown to interact with Ndr kinases.[23,38,39] It has been proposed that human kinases Ndr1/2 complex with both hMob1A/B and hMob2 in a manner stimulated by okadaic acid.[22,39–42] Notably, these studies report hMob1A/B binding to Ndr, an interaction

that does not occur in yeast homologues Cbk1 and Mob1; this is complicated by hMob2's interaction with hMob1A/B,[43] also observed in *S.cerevisiae*.[44] Human Mob1 has been reported to bind Ndr1 only when phosphorylated by Mst2, whereas binding to Lats1 is independent of phosphorylation.[42] Conversely, human Lats1/2 cannot bind Mob2 similar to Sid2/Mob2 in *S.pombe,*[23,39] and the nature of this observation remains an open question. A similar phenomenon has been observed in *Drosophila,*[45,46] with the Ndr kinase tricornered (Trc) interacting with *Drosophila* dMob1 (Mats).

Ndr/Lats kinases have a unique 70-80 amino acid long N-terminal region (NTR) preceding their AGC-type kinase domain responsible for Mob cofactor binding. We co-crystallized Mob2 with the NTR of Cbk1 to better understand the kinase-cofactor interface. In the light of this new structure it became clear that the lower resolution electron density map at the NTR in the full Cbk1-Mob2 complex, where the Cbk1 construct also contained its AGC-type kinase domain in addition to the NTR, had been partially misinterpreted.[47] In the present study we collected better resolution crystallographic data on the full Cbk1-Mob2 complex and combined this with the higher resolution model of the Cbk1^{NTR}-Mob2 complex. In the revised model NTR adopts a more helical structure comprised of two helices (αMobA and αMobB) and the peptide backbone of the Cbk1 NTR forms a V-shaped bihelix similar to human Lats1-Mob1[48,49] and Ndr-Mob1.[50] Furthermore, we revised the Cbk1-Mob2 structure[47] and show that highly conserved residues at the NTR-Mob interface may also participate in crucial interactions with the kinase's hydrophobic motif (HM). To compare the Cbk1-Mob2 binding interface with Dbf2-Mob1, we solved the structure of Dbf2^{NTR} bound to Mob1. We show that while Dbf2 binds to Mob1 through an architecture nearly identical to human Lats1, Cbk1 interacts with Mob2 through several *S.cerevisiae*-specific motifs, suggesting greater structural variety of Ndr kinases within the eukaryotic world. We further show Dbf2 and Cbk1 bind specifically to the Mob1 and Mob2 cofactors, forming isolated Dbf2-Mob1 and Cbk1-Mob2 complexes. A conserved docking motif identified in the Mob1/2 structures contributes strongly to the molecular recognition between the kinase and the cofactor; mutation of this motif can form non-cognate complexes Dbf2-Mob2 and Cbk1-Mob1 as well as perturb the binding

affinity of the cognates. We hope to shed light on the structure and function of these pathways.

Results

A higher-resolution Cbk1^{NTR}-Mob2 structure revises the previously published Cbk1-Mob2 model

As reported previously,[25] monomeric Mob2 does not purify in an *E.coli* overexpression system. To produce useful amounts of this protein, we engineered a mutant Mob2 $^{V148C\ Y153C}$ which recapitulates the zinc-binding motif found in both *S.cerevisiae* Mob1 and most metazoan Mob2 homologues. This mutant can be stably expressed and purified. Unless otherwise noted, all interaction data, as well the Cbk1^{NTR}-Mob2 crystal structure, were obtained using this mutant.

The previously published Cbk1-Mob2 structure offered new insight into the architecture of kinase-coactivator binding, albeit this structure could be determined only at 3.3 Å resolution.[47] To further understand the interaction interface between the kinase and its Mob2 coactivator, we solved the structure of the Cbk1 ^{NTR} (Cbk1$^{251-351}$) bound to Mob2$^{45-287}$ to 2.8 Å resolution (Figure 1A,B). Unexpectedly, Cbk1^{NTR} formed a two-helix bundle distinct from the single helix-strand structure we observed previously (Figure 1A). Both Mob2 and Cbk1^{NTR} were conformationally similar to the previously solved Lats1 structure (Figure 1C),[48,49] as well as the Ndr1 structure.[50] Also observed was an N-terminal strand 259-277 with an array of contacts on the back of Mob2 (Figure 1D). Due to substantial structural similarities with Lats1, we adopted the interface I/II/III notation utilized previously to describe the interaction (Figure 1E).[48]

Since the publication of the full Cbk1-Mob2 crystal structure (3.3 Å), three higher resolution crystal structures were determined where Mob coactivator proteins were complexed with the unique N-terminal extension of two Ndr/Lats kinases.[48–50] These recent structures and the newly solved Cbk1^{NTR}-Mob2 complex presented in this study added greatly to our understanding on the structural basis of Ndr/Lats coactivator binding. These new findings called for a revision on the full Cbk1-Mob2 crystallographic model. We used improved crystallographic data to remodel our previous incomplete

model and also used the new NTR structures (containing the N-linker and two long helices of the αMob region) in crystallographic model building. Using the high resolution templates of yeast Mob2 and the Cbk1^{NTR} we were able to refine the model with much greater fidelity. The new model showed similar conformation compared to other bound NTR structures with a helical N-linker (αMobA) which eventually corrected our original 14 residue long register shift in the first helical binding region (αMobB). In addition, we were able to resolve the C-terminal extension of the hydrophobic motif which adopts a helical conformation (αHM).We further resolved a novel interaction between the highly conserved Arg-752 of the αHM and Glu-336 of the NTR which may explain the unusual phosphorylation-independent binding of the Cbk1(HM) to the kinase.[47] This important regulatory region now fills up the HM binding slot between the αMob and the core of the kinase domain (Figure 2). Furthermore, the phosphorylated Thr-743 is positioned above the conserved Arg-343 of the NTR, suggesting a role of these amino acids in kinase activation. As all these residues are conserved, this likely represents a structure commonly found in Ndr/Lats kinases across the eukaryotic world. Additional data and modeling based on the higher resolution crystal structure of the Cbk1^{NTR}-Mob2 complex greatly improved the electron density map of the full Cbk1-Mob2 complex. This enabled us to correct smaller inaccuracies of our former low resolution model such as the conformation of the DFG motif important in kinase activation as well as the N-terminal extension of Mob2. The full Cbk1-Mob2 was crystallized in the presence of small docking peptide from Ssd1.[47] This peptide, however, could not be traced in the old crystal structure, but the improved map clearly showed additional electron density close to the peptide binding groove previously identified by in silico docking.[47] Because the observed density was close to Phe-447, Trp-444 and Tyr-687–mutation of which interfered with peptide binding–but far from Phe-699–mutation of which did not affect binding–, we concluded that the actual Cbk1 docking groove was now successfully identified. This somewhat deeper pocket on the Cbk1 surface accepts one of the pivotal phenylalanine of the FxFP consensus docking motif (Figure 2).

Dbf2-Mob1's interaction architecture is similar to Lats1-hMob1, but distinct from Cbk1-Mob2

While a majority of the yeast Mob1's biochemical properties have been derived from temperature sensitive mutations discovered in Mob1,[24,25,27] the interaction interface with Dbf2 remains poorly characterized. To more completely understand this interaction and compare it with its Cbk1 and Lats1 homologues, we crystallized Mob1$^{79-314}$ bound to Dbf2^{NTR} (Dbf2$^{85-173}$) and solved the structure at 3.5 Å resolution (Figure 3A). We found that Mob1 in complex with Dbf2 is nearly identical to the unbound (apo) Mob1 structure solved previously.[44] The H0 helix observed in dimeric Mob1 structure was also not observed in our model.[44] We crystallized Dbf2^{NTR}-Mob1 in the presence of aggregation inhibitors which may disrupt the H0-Mob1 core interaction, and H0 may be exposed to the solvent and disordered. Dbf2^{NTR} formed a bihelical bundle conformationally similar to both Lats1^{NTR} and Cbk1^{NTR}, though lacking the helical kink observed in some Lats1 structures.[49]

Given Dbf2's general grouping into the Lats subfamily,[4] we sought to compare it to the previously solved Lats1 structures. Similar to Lats1,[48,49] Dbf2 arginines Arg-125 and Arg-128 (RxxR at Interface II, see Figure 1E) protrude from αMobA and "sandwich" Glu-161 on αMobB (Figure 3B, left), with Arg-125 facing Mob1 akin to interface II in Lats1.[48] Arg-125 further bridges with Mob1 Glu-151, conserved in Mob1-subfamily kinases,[25] and with αMobB His-162, not found in other kinases (Figure 3B, right). All residues are homologous to Arg-657, Arg-660, and Glu-689 in Lats1 as described previously (Supplementary Figure 1).[48,49] Furthermore, the allele *Mob1-77* (E151K) was shown to cause cell-cycle arrest at non-permissive temperature and maps within Mob1's H1-H2 loop. [24,25,27]

The second "core" Dbf2 interaction domain, analogous to Lats1 interface III, consists of four basic residues; Arg-166 and Arg-169 contact Mob1 Glu-155, with Arg-168 interacting with Asp-117 to stabilizing the αMobA/B helical bundle (Figure 3B, left). The geometry of the Mob1 Glu-155 to Arg-166/168 interaction is strongly conserved; both Lats1 and Cbk1 bind to cognate Mobs in a nearly identical geometry (Supplementary Figure 1). This region maps on to interface III described previously

in Lats1-Mob1.[48] Curiously, Dbf2 His-162 replaces a Ser/Thr at this position in metazoan Ndr/Lats kinases and may be important for binding Mob in Lats and Ndr (Supplementary Figure 1).[22,39,48,49,51–53]

We next verified the structure by performing interaction assays with point mutants in conserved residues identified in the crystal structures. We found Dbf2 and Cbk1 NTRs to strongly form aggregates when purified, a pattern previously observed in human Lats^{NTR},[48,49] and failed to produce direct interaction data. We note, however, that ITC data for the human Ndr-Mob1 interaction has been obtained, though the oligomeric state of the Ndr used is not specified.[50] This aggregation pattern also applies to mutant NTR-Mob1 complexes with weak cohesion between the subunits. We found that fusion to maltose binding protein (MBP) dampens the aggregation of unstable Ndr/Lats-Mob complexes and permits detection of interactions when co-expressed with Mob in a bacterial system. MBP-Dbf2^{NTR} Mob1 interaction assays demonstrated that Dbf2 Arg-125, Arg-166, and Arg-169 contribute strongly to the interaction, as predicted by the crystal structure (Figure 3C, lanes 2, 5, and 7). Mutation of non-Mob-binding Arg-128, Glu-161, and Arg-168 either ablated or abolished the interaction, indicating integrity of the NTR is crucial to formation of the complex similar to the intra-αMob interaction between Lats1 Arg-660 and Glu-689 (Figure 3C, lanes 3, 4, and 6).[48] Interestingly, Lys-171 does not participate in Mob1 binding despite strong charge conservation across the eukaryotic world (Figure 3C, lane 8). Thus, interacting residues in the Dbf2-Mob1 structure participate in binding.

The revised Cbk1-Mob2 structure reveals an interface distinct from Lats/Dbf2

Despite the volume of literature on the Ndr residues required for Mob1 interaction,[22,23,39–41,48–50,53–55] little has been published on the analogous interface with Mob2. We analyzed the Cbk1^{NTR}-Mob2 structure to understand the Ndr-Mob2 interaction. Cbk1's conserved residues Arg-304 and 307 (RxxR, at Interface II) have similar geometry to Lats1 Arg-657 and 660,[48,49] with important differences (Figure 4A). While Cbk1 Arg-307 bridges with Glu-336 on αMobB similar to the inter-helical cohesion between Lats1 Arg-660 and Glu-689, Cbk1 Arg-304 does not interact with Mob in the crystal structure as Lats1

Arg-657 and Dbf2 Arg-125 do (Figure 4A), instead being sterically pushed towards the center of Mob2 by the hydrophobic Val-120 and Cbk1 Leu-340 (Figure 4C, left). Replacing this interaction, Mob2 Lys-118 and Tyr-119 extend from the H1-H2 loop and contact Cbk1 Glu-312, forming a salt bridge and a hydrogen bond, respectively, and laying in a pocket formed at the intersection of the two αMob helices (Figure 4C, right). Glu-312 is not conserved in Dbf2, but found in other known Ndr/Lats-subfamily kinases in metazoans. Cbk1 Arg-341 and Arg-344 bind Mob2 Glu-124 forming interface III also found in Lats1 and Dbf2 (Figure 4B). Thus, Cbk's interaction with Mob2 partially occurs through an interaction distinct from Lats1/Dbf2 (Figure 4D).

Mob1 and Mob2 exhibit intrinsic binding specificity for their cognate kinases

The kinase-Mob binding specificity in *Saccharomyces cerevisiae* remains poorly characterized. Drawing from *Schizosaccharomyces pombe*,[35,36] we hypothesized yeast kinases Dbf2 and Cbk1 bind Mob1 and Mob2 to form cognate Dbf2-Mob1 and Cbk1-Mob2 complexes without cross-interaction. We tested binding specificity by bacterially co-expressing the Dbf2 and Cbk1 NTR domains with Mob1/2. We observed cognate complexes Dbf2-Mob1 and Cbk1-Mob2 bound (Figure 5A, lanes 1-4), with the non-cognate complex Cbk1-Mob1 interacting weakly (Figure 5A, lane 2) consistent with data from *Schizosaccharomyces pombe*.[35] Similar results were obtained yeast two-hybrid (Supplementary Figure 2). Coexpression of histidine-tagged Dbf2 and Cbk1^{NTR} from a bi-cistronic plasmid, which is more sensitive to reductions in binding affinity, yielded only cognate complexes (Figure 5B). In conclusion, Dbf2 and Cbk1 bind to cognate cofactors Mob1 and Mob2, with limited cross-specificity.

The Cbk1 αNT contributes strongly to Cbk1-Mob2 binding specificity

The Cbk1^{NTR}-Mob2 crystal structure revealed that a non-conserved strand Cbk1$^{259-277}$, required for expression of the full-length Cbk1-Mob2 complex, formed contacts with the back of Mob2 (see Figure 1D). Preliminary mutational analysis of the Cbk1^{NTR} in interfaces II and III failed to abolish

binding to Mob2, further suggesting an alternative binding site (data not shown). Indeed, truncation of Cbk1 to a minimal construct Cbk1$^{251\text{-}303}$ (Cbk1 $^{\alpha NT}$), containing this strand and first 27 amino acids of the αMobA helix, was sufficient to bind zinc-binding Mob2 with wild-type affinity despite the lack of the conserved electrostatic interactions found in Dbf2/Lats interfaces II and III (Figure 5A, lane 5-8). Furthermore, Cbk1 $^{\alpha NT}$ expressed with Mob2 lacking the zinc binding mutation is sufficient to express the coactivator solubly, suggesting a novel Cbk1-Mob2 interaction motif replaces the metal binding site (data not shown). In contrast, Dbf2$^{85\text{-}124}$(Dbf2 $^{\alpha NT}$) cannot bind Mob1 or Mob2 and is rapidly degraded, suggesting the bihelical motif is required for stabilizing the Dbf2 NTR (Figure 5A, lanes 5, 7).

The Mob kinase restrictor motif (KRM) constrains kinase binding to a single cofactor

Despite differences in sequence, all crystallized Ndr/Lats kinases interact with Mob through a conserved loop H1-H2, previously described in hMob1A to connect helices 1 and 2 and interact with Lats1 (Supplementary Figure 3A,B).[25,48,49] Alignment of the H1-H2 domains of yeast and human Mob reveal a highly conserved sequence (L,P)xxx(D,N) which separates Mob1 and Mob2 subfamilies (Supplementary Figure 4). In yeast Mob1, the conserved proline Pro-148 is hypothesized to stabilize the H1-H2 loop,[25] with the solvent-exposed Asp-152 initiating helix 2. Mutations in Pro-148 lead to loss of Mob1 function.[25] Importantly, the three variable residues are subfamily-specific, with xGE representing Mob1 and Mob2 having no strongly conserved alignment (Supplementary Figure 4). We named this tripeptide the kinase restrictor motif (KRM) and posited it strengthens or otherwise effects kinase-Mob binding specificity.

We sought to determine the role of this motif in the kinase-Mob interaction. Mob1 and Mob2 with sequences swapped between proteins were co-expressed with stabilized MBP fusions of Dbf2 and Cbk1^{NTR}. The Mob1 ^{Mob2KRM} (Mob1$^{R149K\ G150Y\ E151V}$) mutant bound its cognate Dbf2 weakly and the non-cognate Cbk1 with greater affinity when compared with wild-type (Figure 5C). The Mob2 ^{Mob1KRM} (Mob2 $^{K118R\ Y119G\ V120E}$) chimera bound Dbf2, an interaction not reported in *S. pombe, S. cerevisiae,* or in the

human Lats1 (Figure 5D).[23,35,39,56] Thus, exchange of this region between Mob cofactors can confer or enhance their ability to bind non-cognate Ndr/Lats kinases.

We next determined if the interaction of the *S.cerevisiae* Mob KRM mutants with the Ndr/Lats^{NTR} were consistent with the established Ndr/Lats-Mob binding architectures and not artifactual or otherwise due to oligomerization or nonspecific interactions within the complex. Mob1 ^{Mob2KRM} and Mob2 ^{Mob1KRM} were expressed with MBP-fused Dbf2 and Cbk1 mutants with mutations in conserved residues in interfaces II and III (Supplementary Figure 5). Alanine substitutions for Dbf2 Arg-125 and Arg-128 ablated binding to chimeric Mob2 ^{Mob1KRM}, similar to that observed in Mob1 and consistent with the Dbf2-Mob1 and Lats1-hMob1 crystal structures (Supplementary Figure 5A, lanes 4-5).[48,49] Importantly, substitution of Cbk1 Arg-304 for alanine does not affect binding of Cbk1 to Mob1 ^{Mob2KRM}, consistent with this residue's lack of Mob interaction and demonstrating Cbk1's binding is through a Mob2-like binding interface (Figure 4C, and Supplementary Figure 5B, lane 4). Mutations in interface III's conserved Dbf2/Cbk1 Arg-166/341 and Arg-169/343 residues, found in all known Lats/Ndr kinases, further ablates the interaction (Supplementary Figure 5A,B, lanes 7-9). These findings suggest the Mob KRM interacts through the NTR in a manner consistent with its placement in the crystal structure.

Discussion

Ndr/Lats kinase activation: the role of HM phosphorylation and Mob binding

Phosphorylation at the HM on Thr-743 by an upstream kinase activates Cbk1 and the C-terminal activation loop (AL) region harbors an auto-phosphorylation site (Ser-570) which is required for full activation. This residue is placed near interface III of the Cbk1^{NTR}, being positioned close to the highly conserved basic residues in that region such as Arg-343 (Figure 2). We further note that the position of this residue is possibly fixed by the Mob2 interaction, and may replace the basic binding pocket found in most AGC kinases. We suggest that this region may common in Ndr/Lats kinases due to the high

similarity between the Cbk1-Mob2 structure and previously published complexes of Lats1^{NTR}-Mob1 as well as our Dbf2^{NTR}-Mob1 structure (Figure 4).[48,49]

In order to gain insight into how phosphorylation at these two regulatory sites may promote kinase activity, we performed MD simulations on the complex to address the possible allosteric role of AL and particularly HM phosphorylation; as the new Cbk1^{NTR}-Mob2 crystal structure necessitated the revision of the activation model that we had formerly put forward.[47] For MD simulations a hybrid model was constructed using the new, corrected Cbk1-Mob2 crystal structure and PKB/Akt structures (PMID: 12434148). In contrast to our earlier findings, where we relied on a less complete Cbk1-Mob2 crystal structure to construct an MD starting model, the new simulations did not indicate long range movements at αMobB (previously referred to as N-linker) between αMobA and the AGC kinase core. In the light of the corrected model, however, this is now not surprising. In the old model the HM region could only be partially traced and the amino acid register of the αMobA helix was misinterpreted. In the revised crystallographic model, the full HM region became visible and the register at the N-terminus was corrected.

Although the new MD simulations indicated some small-range differences regarding the movements of critical Cbk1^{NTR} arginine residues directly contacting the phosphorylated side chain of Thr-743 (e.g. Arg-343, located at Interface III) in the conformational dynamics of the non-phosphorylated and phosphorylated complexes, this computational approach failed to reveal the exact mechanistic role of Ser-570 and Thr-573 phosphorylation in Cbk1 activation: (1) biochemically feasible modeling of the critical αC segment became possible only if main-chain restraints were applied, (2) trajectories even for long (~1 μM) simulations were too sensitive to small differences in the starting models as the outcome varied depending on what parts of the models were allowed to move freely or restraint, or if the models contained ATP or Mg.ATP for example (Supplementary Figure 6). Despite of this, tentatively, the Cbk1 HM region may promote the ordering of αC in the phosphorylated complex and thus influences activity through this kinase region known to be frequently involved in allosteric

regulation. Overall, our structural and MD analysis is consistent with a mechanistic model where Ser-570 phosphorylation at the activation loop and particularly Thr-743 phosphorylation at the HM promote the optimal positioning of the otherwise flexible αC. This mechanism clearly resembles to how HM phosphorylation and binding at the so-called PIF pocket affects the activity of other better known AGC kinases (PMID: 12434148) (Figure 6).

Evolutionarily conserved features of the Ndr/Lats kinase-coactivator interface

In humans, Lats kinases restrain cell proliferation by keeping the YAP/TAZ transcription factors out of the nucleus. Ablation of signaling within the pathway, such as reductions in Ndr/Lats catalytic activity or 14-3-3 levels, which promote YAP/TAZ cytosolic sequestration can cause cell overgrowth and transformation.[57] All solid tumors appear to circumvent hippo pathway inhibition of YAP/TAZ. Our findings identify conserved basic amino acids in the NTRs of Ndr/Lats kinases that are probably essential for their functionally critical interaction with Mob cofactors. Notably, mutations affecting these basic amino acids in human Lats1 and 2 have been linked to cancers: R657C, R694C, and R697G mutations in Lats1 strongly correlate with uterine, ovarian, and papillary renal cell cancers, and Lats2 R623W correlates with melanomas.[58] We suggest that these Lats1 and 2 alleles have weakened Mob1 binding, disrupting cofactor interaction and the complex's function.

Dbf2 and Cbk1 are conserved AGC kinases in the Ndr/Lats family and are evolutionarily related to their human counterparts. The conserved arginines on the αMobA and B helices of Dbf2, Cbk1, and Lats contain a conserved RxxR motif (see Figure 1E). Dbf2/Lats uses this motif to bind its Mob factor, whereas Cbk1 does not appear to. While the second arginine appears to electrostatically cohere the αMob helices, the function of Cbk1's Arg-304 remains unknown, as it does not bind Mob2. However, Cbk1 Arg-304 may have some role in stabilizing the HM binding site in the kinase-coactivator complex as $Cbk1^{HM}$ Arg-746 interacts electrostatically with the conserved Glu-336 which is coordinated by the RxxR of $Cbk1^{NTR}$ (Supplementary Figure 3B). Mob1 binds Dbf2 RxxR (involving Arg-125 and Arg-128)

directly to form interface II (Figure 4A), suggesting roles for the cofactor in kinase regulation through modulation of the HM binding site if the structures are homologous.

Do metazoan Ndr kinases exhibit Mob coactivator specificity?

Ndr's interaction with hMob1 has been published,[37] and may be dependent on the phosphorylation of hMob1 Thr-74.[41,42] Mob1 Ser-174 in *S.cerevisiae* is homologous with this residue, though its phosphorylation state is unknown. This non-cognate interaction has not been reproducibly observed in the *S.pombe* or *S.cerevisiae* model systems. We find that Cbk1 strongly binds Mob2 *in vitro*, and while it can associate with wild-type Mob1 this interaction is weak and unstable.

Mutations in interfaces II and III of Ndr1^{NTR} can abrogate binding with hMob1, but not hMob2, suggesting binding to Ndr1 occurs through distinct mechanisms.[39] Whether the observed interaction is direct or through an adapter has not been determined, though point mutations in the NTR suggest binding uses homologous residues to Lats1-hMob1.[22,23,25,48,54] Human hMob1 has been shown to interact with hMob2,[43] an interaction also observed in *S.cerevisiae*[44] by as well as in our own hands (data not shown), suggesting a potential oligomerization mechanism for the cofactors. Further research will be required to fully elucidate the nuances of these interactions.

The ability of human Mob2 to "out-compete" Mob1 for binding to Ndr1 as reported by Kohler et al. is consistent with the observed strength of the Cbk1-Mob2 interaction.[39] No mutation in Ndr^{NTR} is capable of abrogating binding to Mob2,[39] a phenomenon observed with Cbk1 in the hands of the authors as well. Mob1 localizes to spindle pole bodies, but not the bud neck, in the absence of Dbf2;[26] the non-Dbf2-binding *Mob1-77* mutant has a similar effect.[8] In contrast, Mob2 in the absence of Cbk1 displays a completely diffuse localization pattern consistent with degradation in the absence of the stabilizing Cbk1^{NTR};[19,20] this is likely due to the strand of Cbk1 $^{\alpha NT}$ (Cbk1$^{259-277}$) stabilizing Mob2 (Figure 1D). As this strand appears to not exist in Ndr, it may be difficult to draw parallels between human and *S.cerevisiae* biochemistry within the Ndr/Lats paradigm.

Kinase restrictor motif of Mob plays a key role in defining the specificity of kinase-coactivator interactions

Alignment of Mob cofactor protein sequences display subfamily-specific sequences which might divide Mob1 from Mob2 and thus impart specificity on kinase binding (Supplementary Figure 4). The three amino acids identified as the KRM extend from the N-terminus of Mob helix I and orient towards the predicted kinase interaction surface in Mob structures solved previously.[25,44,59] In Ndr/Lats^{NTR}-Mob, the KRM lays into a binding cleft in the NTR (Supplementary Figure 3A). Many inactivating mutations in *S.cerevisiae* and human Mob1 map to this motif or residues surrounding it.[24,25,48]

Comparing the KRMs of eukaryotic Mob1 and 2 subfamilies may reveal similarities in cofactor function. Mob1's high conservation in this region is consistent with its generally conserved role in binding Lats subfamily kinases and in cell cycle exit. Mob2 is more diverse, potentially reflecting the larger variety of functions performed by the Ndr subfamily of kinases in eukaryotic systems. Human Mob2 may interact with Ndr through Arg-48 and Glu-49 of its KRM. In contrast, *Drosophila* Mob2, which contains Ala/Gly in the place of Arg/Glu, may not utilize the motif to bind Tricornered. Such large differences within the normally conserved Ndr-Mob families may explain the difficulty of abolishing the human Ndr1-Mob2 interaction through point mutations at conserved residues in previous work.[39]

In our revised structure the conserved arginines in Cbk1's Mob2-binding NTR (RxxR) associate with Arg-746 in the kinase's C-terminal regulatory hydrophobic motif (HM) (Supplementary Figure 3B). The position of Mob2^{KRM} directly covering the highly conserved HM binding site in Cbk1 suggests a role for regulation. As hMob1/Mob1^{KRM} directly binds the homologous domain through Glu-51/151, we hypothesize Mob1 modulates the conformation of the putative Lats/Dbf2 HM binding region and subsequently controls the kinase.

Our analysis here indicates that the Ndr/Lats^{NTR}-Mob interface is a common structural platform through which kinase-cofactor binding is mediated, however, amino acid variations in key positions

contribute to subgroup and organism-specific differences. While the first Mob crystal structures suggested that a conserved and acidic surface was responsible for interactions with Ndr/Lats through the kinase N-terminus, the reality may be more complex. Some Mob cofactors may bind and activate their cognate kinases through a conserved set of charged residues; others may bind using distal regions and use these residues for activation only, or for alternative functions of Mob. More research is required to elucidate the mechanisms of binding, specificity, and activation of these unique complexes and their role in physiology.

Methods

Expression and Purification of Proteins

To purify the zinc-binding Cbk1^{NTR}-Mob2$^{V148C\ Y153C}$ complex, a modified bi-cistronic pBH4 vector containing His_6-Cbk1 (Cbk1^{NTR}, residues 251-351) and zinc-binding GST-Mob2$^{V148C\ Y153C}$ (residues 45-287) expressed from a single T7 promoter was cloned by ligating Cbk1 residues 251-756 and Mob2 45-287 into the backbone, then mutating Cbk1 Phe-352 to a stop codon using the QuickChange technique (Agilent). Val-148 and Tyr-153 were mutated to cysteine using the same technique. Protein was overexpressed in BL21(DE3) RIL (Agilent) at 37 °C in Terrific Broth (TB) containing 40 μM zinc chloride . After growth to mid-log phase, IPTG was added to 0.2mM and expressed overnight at 37 °C. Cell pellets were lysed by sonication, purified using nickel chromatography, and tags cleaved using Tobacco Etch Virus (TEV) protease overnight on wet ice. Cleaved protein was further purified using a hand-poured SP-Sepharose (GE) column and eluted with a gradient from 50-2000 mM NaCl, then buffer exchanged into 20 mM HEPES pH 7.4, 300 mM NaCl and concentrated to 55 mg/ml.

To purify the Dbf2^{NTR} -Mob1 complex, a bi-cistronic vector containing His_6-Dbf2^{NTR} (85-173) and untagged Mob1 (79-314) expressed from a single T7 promoter was cloned and overexpressed in BL21 (DE3). Mob1 (79-314) contained the N-terminal amino acid sequence ENLYFQGS as a byproduct of cloning. TB cultures containing 40 μM zinc chloride were inoculated, grown to mid-log phase,

induced with IPTG to 0.2 mM, and expressed overnight at 24 °C. Cell pellets were lysed by sonication. Protein was purified using nickel chromatography and cleaved overnight on wet ice using TEV protease. Residual TEV and nickel-binding contaminants were reabsorbed using nickel resin, final protein was then buffer exchanged into 100 mM sodium phosphate pH 7.4, 50 mM KCl, 100 mM L-arginine HCl , and concentrated to 30 mg/ml. L-arginine was present throughout the purification to prevent oligomerization of the complex and did not interfere with nickel chromatography.

Crystallization of Cbk1-Mob2, Cbk1^{NTR}-Mob2, and Dbf2^{NTR}-Mob1 complexes

Ndr/Lats^{NTR}-Mob crystals were obtained at 22.3 °C. Cbk1^{NTR}-Mob2 was crystallized using the hanging-drop method; well solution containing 500 µL 100mM MES/Imidazole pH 6.5, 30 mM CaC_2, 30 mM $MgCl_2$, 12.5% (w/v) PEG1000, 12.5% (w/v) PEG3350, 12.5% (v/v) MPD produced crystals. Dbf2^{NTR}-Mob1 was crystallized using the microbatch method under 200 µL mineral oil (Fisher BioReagents); crystals were obtained in 100 mM Bicine/Tris pH 8.5, 30 mM LiCl, 30 mM NaCl, 30 mM KCl, 30 mM RbCl, 12.5% (w/v) PEG1000, 12.5% (w/v) PEG3350, 12.5% (v/v) MPD. All crystals were frozen in liquid nitrogen without the addition of further cryoprotectant. Cbk1^{NTR}-Mob2 and Dbf2^{NTR}-Mob1 diffracted to 2.80 Å and 3.50 Å, respectively.

Crystallization of the Cbk1-Mob2-Ssd1 complex was identical as previously published.[47] To increase the redundancy of our crystallographic data and to maximize the gained experimental information, we merged two independent datasets collected on this complex (Table 1). This helped to increase the resolution range to 3.15 Å, meaning an additional ~15% experimental data on top of duplicated multiplicity. Data were collected at 100 K on the PXIII beamlines of the Swiss Light Source (Villigen, Switzerland) and at the Advanced Photon Source (Argonne, IL). Data was processed with XDS (doi: 10.1107/S0907444909047337) and the structures of Cbk1^{NTR}-Mob2, and Dbf2^{NTR}-Mob1 complexes were solved by molecular replacement with PHASER (doi: 10.1107/S0021889807021206). The MR search identified single Mob-αMob complexes with a searching model of Lats1-hMob1 (PDB

ID: 5BRK). Structure refinement was carried out using PHENIX (doi:10.1107/S0907444909052925) and structure remodeling and building was performed in Coot (doi: 10.1107/S0907444910007493).

Pull-down experiments

Dbf2 (85-173) and Cbk1 (251-352) were cloned into pMAL-c2x (New England Biolabs) and fused to an N-terminal MBP tag. *S.cerevisiae* Mob1 (79-314) and zinc-binding Mob2 $^{V148C\ Y153C}$ (45-278) were cloned into pET28a (EMD Biosciences). Plasmids were mutated using the QuickChange technique (Agilent). Constructs were co-transformed into BL21(DE3) or BL21(DE3) RIL, grown in TB at 37 °C for two hours, induced with IPTG to 2 mM, and grown overnight at 18 °C or 24 °C. Cell pellets were lysed by sonication and raw protein measured by Bio-Rad Protein Assay (Bio-Rad). Lysates were normalized, incubated with nickel resin (Qiagen) or amylose resin (New England Biolabs), washed twice with 20 mM imidazole, and eluted in 300 mM imidazole (nickel) or by boiling resin in 1X SDS-PAGE loading dye (amylose). Purified protein was separated using 15% SDS-PAGE gels and visualized using an Odyssey infrared imager (LI-COR Biosciences).

Immunoblotting

Bacterial cell lysates normalized in raw protein concentration were separated on 15% SDS-PAGE gels and transferred to polyvinylidene difluoride (PVDF) membranes using Dunn's modified transfer buffer.[60] Blots were blocked using Odyssey Blocking Buffer (LI-COR Biosciences) for 30 minutes and probed with mouse αMBP or rabbit αHis$_6$ antibodies for 1 hour at room temperature. Membranes were washed three times with TBS-T, probed with fluorophore-conjugated IRDye 680LT goat αMouse or IRDye 800CW goat αRabbit (LI-COR Biosciences) for 30 minutes, and washed another three times with TBS-T. Blots were imaged using an Odyssey infrared imager.

Yeast two-hybrid

Plasmids containing the Mob179-314 and Mob245-278 were fused to Gal binding domains and transformed into the Y2H Gold strain. Dbf2 and Cbk1NTR were fused to the Gal activation domain and transformed into Y187. Serial dilutions of cultures were grown on –Leu –Trp –His triple dropout media containing 25mM 3-Amino-1,2,4-triazole (3-AT) until colonies were visible.

Molecular dynamics simulations

MD simulations were carried out as described earlier but using the revised Cbk1-Mob2 crystal structure presented in this study.[47] Since the αC of Cbk1 was not resolved in the crystal structure, homology modeling was used to build this region based on the structure of activated PKB (PMID: 12434148). Furthermore, the activation loop segment with the Ser-570 autophosphorylation site as well as the DFG loop of the Cbk1-Mob2 complex was remodeled to make it adopt a similar structure as it had formerly been observed in other activated AGC kinases.

Structure deposition

The crystallographic models of the Dbf2(NTR)-Mob1, Cbk1(NTR)-Mob2 and the revised Cbk1-Mob2-pepSsd1 complexes have been deposited in the Protein Data Bank with accession codes: 5NCN, 5NCM and 5NCL, respectively.

Funding

This work was supported by the National Institute of Health [grant number 5R01GM084223-08]. A.R. is the recipient of the Lendület grant from the Hungarian Academy of Sciences (LP2013-57). The work was also supported by a grant from the Hungarian Research Fund (OTKA NN 114309). The content is solely the responsibility of the authors and does not necessarily represent the official views of the National Institutes of Health.

We acknowledge staff and instrumentation support from the Structural Biology Facility at Northwestern University, the Robert H Lurie Comprehensive Cancer Center of Northwestern University and NCI CCSG P30 CA060553.

This research used resources of the Advanced Photon Source, a U.S. Department of Energy (DOE) Office of Science User Facility operated for the DOE Office of Science by Argonne National Laboratory under Contract No. DE-AC02-06CH11357. Use of the LS-CAT Sector 21 was supported by the Michigan Economic Development Corporation and the Michigan Technology Tri-Corridor (Grant 085P1000817).

References

1. Meng, Z., Moroishi, T. & Guan, K.-L. Mechanisms of Hippo pathway regulation. *Genes Dev.* **30,** 1–17 (2016).
2. Hergovich, A., Stegert, M. R., Schmitz, D. & Hemmings, B. A. NDR kinases regulate essential cell processes from yeast to humans. *Nat. Rev. Mol. Cell Biol.* **7,** 253–264 (2006).
3. Emoto, K. The growing role of the Hippo–NDR kinase signalling in neuronal development and disease. *J. Biochem. (Tokyo)* **150,** 133–141 (2011).

4. Hergovich, A. The Roles of NDR Protein Kinases in Hippo Signalling. *Genes* **7,** 21 (2016).
5. Zhao, B. *et al.* Inactivation of YAP oncoprotein by the Hippo pathway is involved in cell contact inhibition and tissue growth control. *Genes Dev.* **21,** 2747–2761 (2007).
6. Hergovich, A. & Hemmings, B. A. Hippo signalling in the G2/M cell cycle phase: Lessons learned from the yeast MEN and SIN pathways. *Semin. Cell Dev. Biol.* **23,** 794–802 (2012).
7. Yoshida, S. & Toh-e, A. Regulation of the localization of Dbf2 and mob1 during cell division of saccharomyces cerevisiae. *Genes Genet. Syst.* **76,** 141–147 (2001).
8. Frenz, L. M., Lee, S. E., Fesquet, D. & Johnston, L. H. The budding yeast Dbf2 protein kinase localises to the centrosome and moves to the bud neck in late mitosis. *J. Cell Sci.* **113,** 3399–3408 (2000).
9. Mah, A. S., Jang, J. & Deshaies, R. J. Protein kinase Cdc15 activates the Dbf2-Mob1 kinase complex. *Proc. Natl. Acad. Sci.* **98,** 7325–7330 (2001).
10. Visintin, R. & Amon, A. Regulation of the Mitotic Exit Protein Kinases Cdc15 and Dbf2. *Mol. Biol. Cell* **12,** 2961–2974 (2001).
11. Rock, J. M. *et al.* Activation of the Yeast Hippo Pathway by Phosphorylation-Dependent Assembly of Signaling Complexes. *Science* **340,** (2013).
12. Hotz, M. & Barral, Y. The Mitotic Exit Network: new turns on old pathways. *Trends Cell Biol.* **24,** 145–152 (2014).
13. Bardin, A. J. & Amon, A. MEN and SIN: what's the difference? *Nat. Rev. Mol. Cell Biol.* **2,** 815–826 (2001).
14. Nelson, B. *et al.* RAM: A Conserved Signaling Network That Regulates Ace2p Transcriptional Activity and Polarized Morphogenesis. *Mol. Biol. Cell* **14,** 3782–3803 (2003).
15. Racki, W. J., Bécam, A.-M., Nasr, F. & Herbert, C. J. Cbk1p, a protein similar to the human myotonic dystrophy kinase, is essential for normal morphogenesis in Saccharomyces cerevisiae. *EMBO J.* **19,** 4524–4532 (2000).

16. Bidlingmaier, S., Weiss, E. L., Seidel, C., Drubin, D. G. & Snyder, M. The Cbk1p Pathway Is Important for Polarized Cell Growth and Cell Separation in Saccharomyces cerevisiae. *Mol. Cell. Biol.* **21,** 2449–2462 (2001).
17. Mazanka, E. *et al.* The NDR/LATS Family Kinase Cbk1 Directly Controls Transcriptional Asymmetry. *PLOS Biol* **6,** e203 (2008).
18. Mazanka, E. & Weiss, E. L. Sequential Counteracting Kinases Restrict an Asymmetric Gene Expression Program to early G1. *Mol. Biol. Cell* **21,** 2809–2820 (2010).
19. Colman-Lerner, A., Chin, T. E. & Brent, R. Yeast Cbk1 and Mob2 Activate Daughter-Specific Genetic Programs to Induce Asymmetric Cell Fates. *Cell* **107,** 739–750 (2001).
20. Weiss, E. L. *et al.* The Saccharomyces cerevisiae Mob2p–Cbk1p kinase complex promotes polarized growth and acts with the mitotic exit network to facilitate daughter cell–specific localization of Ace2p transcription factor. *J. Cell Biol.* **158,** 885–900 (2002).
21. Voth, W. P., Olsen, A. E., Sbia, M., Freedman, K. H. & Stillman, D. J. ACE2, CBK1, and BUD4 in Budding and Cell Separation. *Eukaryot. Cell* **4,** 1018–1028 (2005).
22. Bichsel, S. J., Tamaskovic, R., Stegert, M. R. & Hemmings, B. A. Mechanism of Activation of NDR (Nuclear Dbf2-related) Protein Kinase by the hMOB1 Protein. *J. Biol. Chem.* **279,** 35228–35235 (2004).
23. Bothos, J., Tuttle, R. L., Ottey, M., Luca, F. C. & Halazonetis, T. D. Human LATS1 Is a Mitotic Exit Network Kinase. *Cancer Res.* **65,** 6568–6575 (2005).
24. Luca, F. C. & Winey, M. MOB1, an Essential Yeast Gene Required for Completion of Mitosis and Maintenance of Ploidy. *Mol. Biol. Cell* **9,** 29–46 (1998).
25. Stavridi, E. S. *et al.* Crystal Structure of a Human Mob1 Protein: Toward Understanding Mob-Regulated Cell Cycle Pathways. *Structure* **11,** 1163–1170 (2003).
26. Luca, F. C. *et al.* Saccharomyces cerevisiae Mob1p Is Required for Cytokinesis and Mitotic Exit. *Mol. Cell. Biol.* **21,** 6972–6983 (2001).

27. Komarnitsky, S. I. *et al.* DBF2 Protein Kinase Binds to and Acts through the Cell Cycle-Regulated MOB1 Protein. *Mol. Cell. Biol.* **18,** 2100–2107 (1998).

28. Mah, A. S. *et al.* Substrate specificity analysis of protein kinase complex Dbf2-Mob1 by peptide library and proteome array screening. *BMC Biochem.* **6,** 22 (2005).

29. Johnston, L. H., Eberly, S. L., Chapman, J. W., Araki, H. & Sugino, A. The product of the Saccharomyces cerevisiae cell cycle gene DBF2 has homology with protein kinases and is periodically expressed in the cell cycle. *Mol. Cell. Biol.* **10,** 1358–1366 (1990).

30. Toyn, J. H. & Johnston, L. H. The Dbf2 and Dbf20 protein kinases of budding yeast are activated after the metaphase to anaphase cell cycle transition. *EMBO J.* **13,** 1103–1113 (1994).

31. Jansen, J. M., Barry, M. F., Yoo, C. K. & Weiss, E. L. Phosphoregulation of Cbk1 is critical for RAM network control of transcription and morphogenesis. *J. Cell Biol.* **175,** 755–766 (2006).

32. Schneper, L., Krauss, A., Miyamoto, R., Fang, S. & Broach, J. R. The Ras/Protein Kinase A Pathway Acts in Parallel with the Mob2/Cbk1 Pathway To Effect Cell Cycle Progression and Proper Bud Site Selection. *Eukaryot. Cell* **3,** 108–120 (2004).

33. Brace, J., Hsu, J. & Weiss, E. L. Mitotic Exit Control of the Saccharomyces cerevisiae Ndr/LATS Kinase Cbk1 Regulates Daughter Cell Separation after Cytokinesis. *Mol. Cell. Biol.* **31,** 721–735 (2011).

34. Mohl, D. A., Huddleston, M. J., Collingwood, T. S., Annan, R. S. & Deshaies, R. J. Dbf2–Mob1 drives relocalization of protein phosphatase Cdc14 to the cytoplasm during exit from mitosis. *J. Cell Biol.* **184,** 527–539 (2009).

35. Hou, M.-C., Guertin, D. A. & McCollum, D. Initiation of Cytokinesis Is Controlled through Multiple Modes of Regulation of the Sid2p-Mob1p Kinase Complex. *Mol. Cell. Biol.* **24,** 3262–3276 (2004).

36. Hou, M.-C., Wiley, D. J., Verde, F. & McCollum, D. Mob2p interacts with the protein kinase Orb6p to promote coordination of cell polarity with cell cycle progression. *J. Cell Sci.* **116,** 125–135 (2003).

37. Hergovich, A. MOB control: Reviewing a conserved family of kinase regulators. *Cell. Signal.* **23,** 1433–1440 (2011).

38. Devroe, E., Erdjument-Bromage, H., Tempst, P. & Silver, P. A. Human Mob Proteins Regulate the NDR1 and NDR2 Serine-Threonine Kinases. *J. Biol. Chem.* **279,** 24444–24451 (2004).

39. Kohler, R. S., Schmitz, D., Cornils, H., Hemmings, B. A. & Hergovich, A. Differential NDR/LATS Interactions with the Human MOB Family Reveal a Negative Role for Human MOB2 in the Regulation of Human NDR Kinases. *Mol. Cell. Biol.* **30,** 4507–4520 (2010).

40. Hergovich, A., Bichsel, S. J. & Hemmings, B. A. Human NDR Kinases Are Rapidly Activated by MOB Proteins through Recruitment to the Plasma Membrane and Phosphorylation. *Mol. Cell. Biol.* **25,** 8259–8272 (2005).

41. Hirabayashi, S. *et al.* Threonine 74 of MOB1 is a putative key phosphorylation site by MST2 to form the scaffold to activate nuclear Dbf2-related kinase 1. *Oncogene* **27,** 4281–4292 (2008).

42. Praskova, M., Xia, F. & Avruch, J. MOBKL1A/MOBKL1B Phosphorylation by MST1 and MST2 Inhibits Cell Proliferation. *Curr. Biol.* **18,** 311–321 (2008).

43. Couzens, A. L. *et al.* Protein Interaction Network of the Mammalian Hippo Pathway Reveals Mechanisms of Kinase-Phosphatase Interactions. *Sci Signal* **6,** rs15-rs15 (2013).

44. Mrkobrada, S., Boucher, L., Ceccarelli, D. F. J., Tyers, M. & Sicheri, F. Structural and Functional Analysis of Saccharomyces cerevisiae Mob1. *J. Mol. Biol.* **362,** 430–440 (2006).

45. He, Y. *et al.* Drosophila Mob Family Proteins Interact with the Related Tricornered (Trc) and Warts (Wts) Kinases. *Mol. Biol. Cell* **16,** 4139–4152 (2005).

46. Giot, L. *et al.* A Protein Interaction Map of Drosophila melanogaster. *Science* **302,** 1727–1736 (2003).

47. Gógl, G. *et al.* The Structure of an NDR/LATS Kinase–Mob Complex Reveals a Novel Kinase–Coactivator System and Substrate Docking Mechanism. *PLOS Biol* **13,** e1002146 (2015).

48. Ni, L., Zheng, Y., Hara, M., Pan, D. & Luo, X. Structural basis for Mob1-dependent activation of the core Mst–Lats kinase cascade in Hippo signaling. *Genes Dev.* **29,** 1416–1431 (2015).

49. Kim, S.-Y., Tachioka, Y., Mori, T. & Hakoshima, T. Structural basis for autoinhibition and its relief of MOB1 in the Hippo pathway. *Sci. Rep.* **6,** (2016).

50. Kulaberoglu, Y. *et al.* Stable MOB1 interaction with Hippo/MST is not essential for development and tissue growth control. *Nat. Commun.* **8,** (2017).

51. Hergovich, A. *et al.* The MST1 and hMOB1 Tumor Suppressors Control Human Centrosome Duplication by Regulating NDR Kinase Phosphorylation. *Curr. Biol.* **19,** 1692–1702 (2009).

52. Stegert, M. R., Tamaskovic, R., Bichsel, S. J., Hergovich, A. & Hemmings, B. A. Regulation of NDR2 Protein Kinase by Multi-site Phosphorylation and the S100B Calcium-binding Protein. *J. Biol. Chem.* **279,** 23806–23812 (2004).

53. Hoa, L. *et al.* The characterisation of LATS2 kinase regulation in Hippo-YAP signalling. *Cell. Signal.* **28,** 488–497 (2016).

54. Hergovich, A., Schmitz, D. & Hemmings, B. A. The human tumour suppressor LATS1 is activated by human MOB1 at the membrane. *Biochem. Biophys. Res. Commun.* **345,** 50–58 (2006).

55. Cook, D., Hoa, L. Y., Gomez, V., Gomez, M. & Hergovich, A. Constitutively active NDR1-PIF kinase functions independent of MST1 and hMOB1 signalling. *Cell. Signal.* **26,** 1657–1667 (2014).

56. Ito, T. *et al.* A comprehensive two-hybrid analysis to explore the yeast protein interactome. *Proc. Natl. Acad. Sci.* **98,** 4569–4574 (2001).

57. Pan, D. The Hippo Signaling Pathway in Development and Cancer. *Dev. Cell* **19,** 491–505 (2010).

58. Yu, T., Bachman, J. & Lai, Z.-C. Mutation analysis of large tumor suppressor genes LATS1 and LATS2 supports a tumor suppressor role in human cancer. *Protein Cell* **6,** 6–11 (2015).

59. Ponchon, L., Dumas, C., Kajava, A. V., Fesquet, D. & Padilla, A. NMR Solution Structure of Mob1, a Mitotic Exit Network Protein and its Interaction with an NDR Kinase Peptide. *J. Mol. Biol.* **337,** 167–182 (2004).

60. Dunn, S. D. Effects of the modification of transfer buffer composition and the renaturation of proteins in gels on the recognition of proteins on western blots by monoclonal antibodies. *Anal. Biochem.* **157,** 144–153 (1986).

Acknowledgments

We thank Kyle Schneider for the Cbk1-Mob2 expression plasmids. We thank Jonathan Hsu for the bi-cistronic plasmid backbone. We acknowledge a grant of computer time from CSCS Swiss National Supercomputing Centre, and NIIF Hungarian National Information Infrastructure Development Institute.

Author Contribution

Eric Weiss conceived this study analyzed data and wrote the manuscript. Attila Reményi analyzed data and wrote the manuscript. Gergő Gógl collected and processed X-ray data, Csaba Hetényi and Mónika Bálint performed MD simulations. Benjamin Parker performed protein biochemistry, collected X-ray data, and wrote the manuscript.

Competing Interests

The authors declare no competing interests.

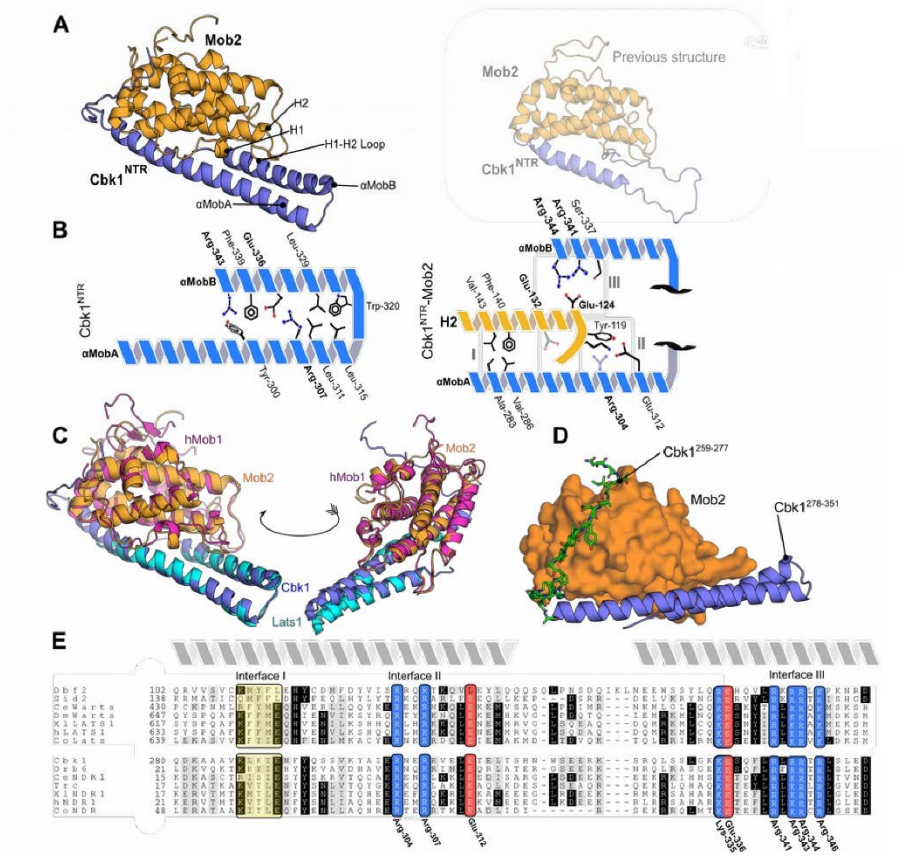

Figure 1 The Cbk1 ^{NTR} -Mob2 complex contains conserved structural motifs

(A) Cbk1 ^{NTR} (251-351, blue) complexed with Mob2 $^{V148C\ Y153C}$ (45-287, orange). The structure of the region taken from the old Cbk1-Mob2 complex including the Cbk1 kinase domain core (PDB ID: 4LQS) is shown faded on the right. (B) The revised Cbk1-Mob2 interaction architecture. Conserved residues are bolded. (C) Cbk1 ^{NTR} -Mob2 (blue/orange) overlayed with Lats1 ^{NTR} -hMob1 (PDB code 5B5W, cyan/purple). (D) Cbk1 residues 259-277 (green, sticks) wrap around the back of Mob2 (orange). (E) Alignment of the Ndr/Lats ^{NTR} regions across eukaryotes. Ce, *Caenorhabditis elegans*; Dm/Wts, *Drosophila melanogaster*; Xl, *Xenopus laevis*; Co, *Capsaspora owczarzaki*. Basic residues, blue; acidic residues, red; hydrophobic regions, yellow. Interfaces I-III equivalent to those described in the Lats1-hMob1 structure are labeled. Conserved residues shown in Cbk1 are labeled.

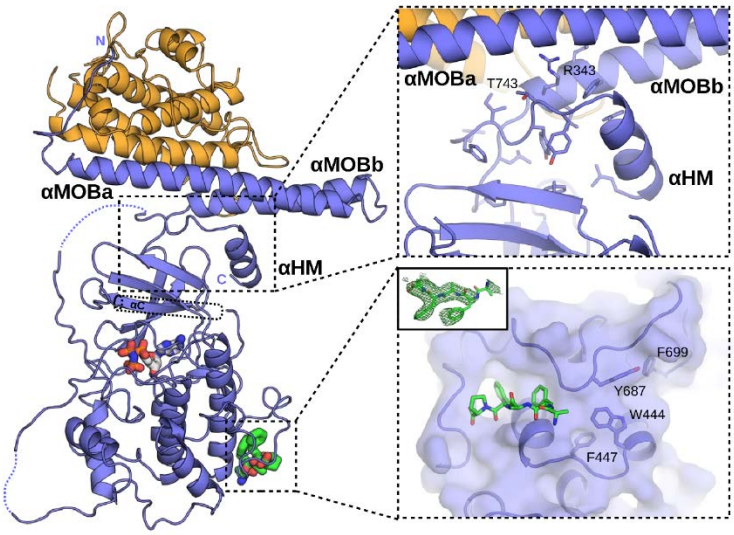

Figure 2 The revised Cbk1-Mob2 crystal structure reveals novel Ndr structural components

The crystal structure of the inactive Cbk1-Mob2 complex was remodeled based on the new Cbk1 ^{NTR} - Mob2 structure. In the new model the co-activator binds to two N-terminal helices (αMobA and αMobB) which together with the top of the kinase domain (β3) form a binding slot for the AGC kinase hydrophobic motif (HM). The C-terminal part of this motif also adopts a helical conformation (αHM). The phosphorylation site on the HM (Thr-743) is next to Arg-343 from αMobB, hinting on the importance of Mob co-activator binding in the allosteric phosphoregulation of the Ndr/Lats kinase domain. Crystallographic model rebuilding also improved the overall quality of the electron density map which enabled us to trace the Ssd1 docking peptide (green sticks). The identified docking groove is placed next to the in silico predicted surface (close to Phe-447, Trp-444, and Tyr-687). The inset shows the simulated annealing Fo-Fc omit map contoured at 2 σ.

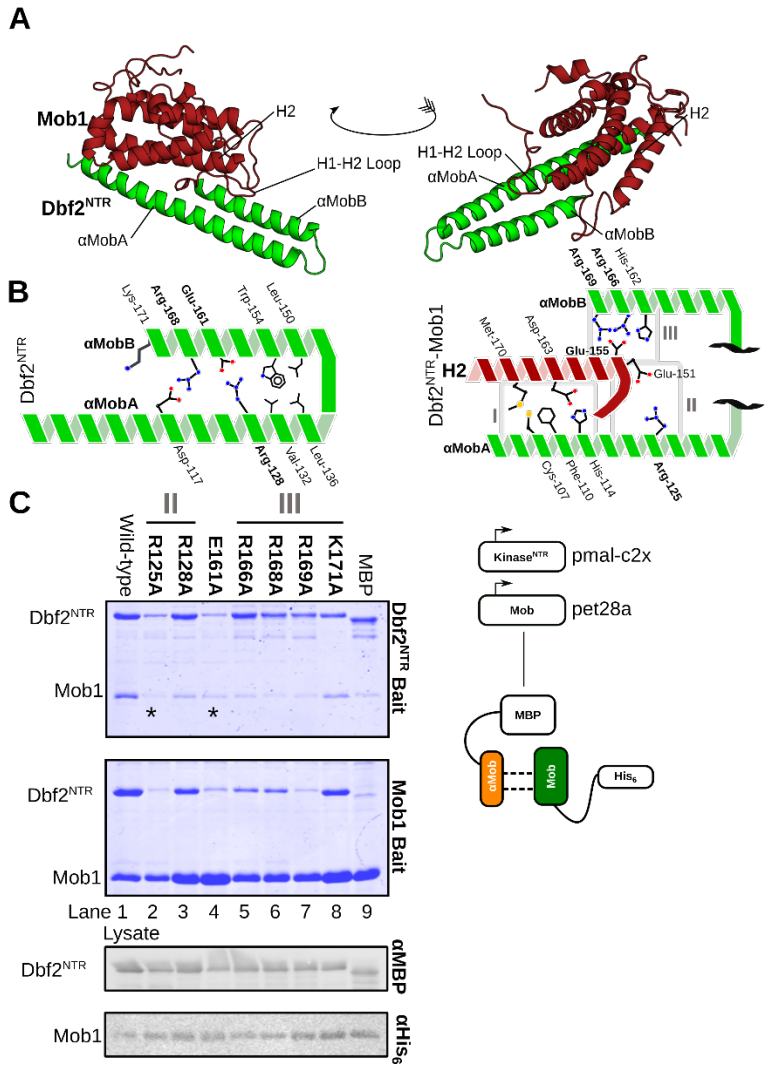

Figure 3 Dbf2 interacts with Mob1 through conserved residues

(A) The structure of Dbf2 ^{NTR} -Mob1 with conserved motifs labeled. Dbf2, green; Mob1, dark red. (B) Interaction architecture of interacting residues within the two Dbf2$^{\alpha Mob}$ helices and between Dbf2 $^{\alpha Mob}$ and Mob1. Conserved residues are shown in bold. (C) BL21(DE3) RIL co-expressing MBP-fused Dbf2 ^{NTR} (85-173) and His_6-fused Mob1 (79-314) followed by purification with amylose and nickel resin. We separated the complexes using SDS-PAGE and stained them with Coomassie. Conserved residues mutated are bolded. Lanes marked (*) adhere poorly to the resin.

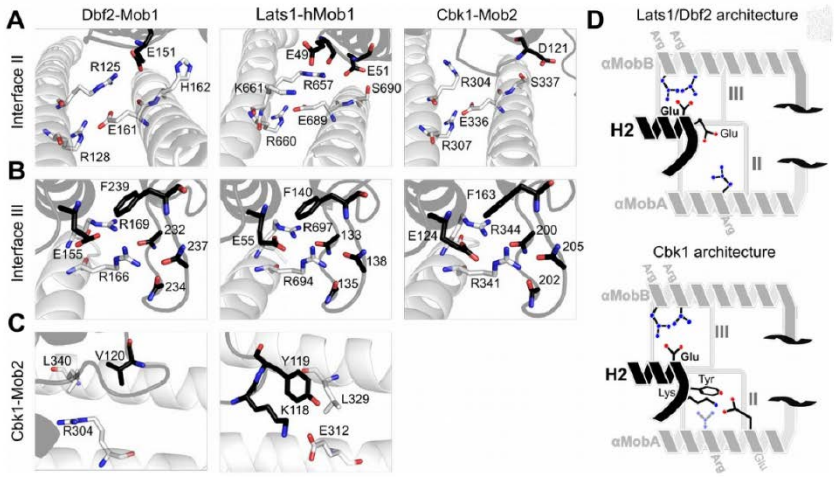

Figure 4 Conserved regions cohere Ndr/Lats ^{NTR} -Mob complexes

Mob is shown in black, kinase ^{NTR} is shown in white. (A) Interface II from Lats1 ^{NTR} -hMob1 (PDB code 5B5W) compared with Cbk1 ^{NTR} -Mob2 and Dbf2 ^{NTR} -Mob1. (B) Comparisons at interface III. (C) More detailed view at Interface II of the Cbk1 ^{NTR} -Mob2 complex showing the orientation of Cbk1 Arg-304 in relation to Leu-340 and Mob2 Val-120 (on the left) and Cbk1 Glu-312 and Mob2 Lys-118, Tyr-119 (on the right). (D) Generalized architecture of Dbf2/Lats1-Mob1 in relation to Cbk1-Mob2.

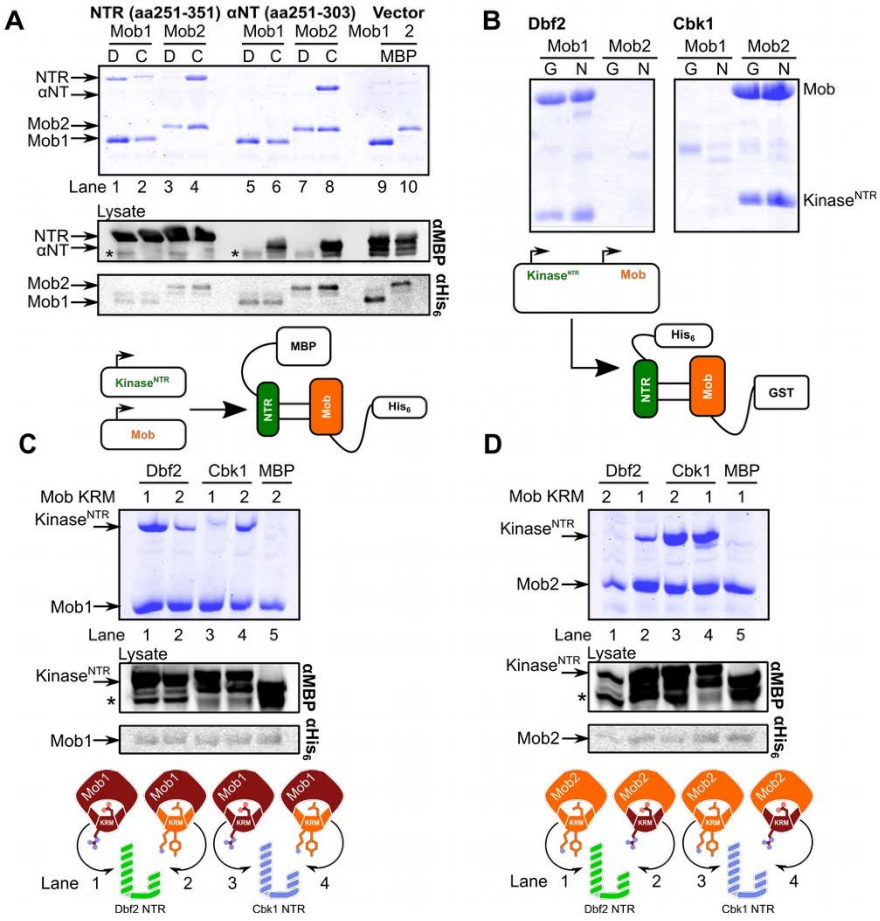

Figure 5 Ndr/Lats-Mob binding is specific and controlled through multiple regions

(A) Dbf2 and Cbk1 form specific complexes with Mob1 and Mob2 *in vitro*. MBP-fused Dbf2^{NTR} (85-173), labeled as "D", and Cbk1^{NTR} (251-351), labeled as "C", were co-expressed with His_6-fused Mob1 (79-314) and Mob2$^{V148C\ Y153C}$ (45-278) in BL21(DE3) RIL, isolated with nickel chromatography, separated with SDS-PAGE, and stained with Coomassie (lanes 1-4). Dbf2^{αNT} (85-124) and Cbk1^{αNT} (251-303) were similarly isolated (lanes 5-8). Lanes 9 and 10 are controls. (B) Complexes of Dbf2^{αNT} and Cbk1^{NTR} with Mob1 and Mob2 were expressed complexes from a single bi-cistronic plasmid in BL21(DE3) and isolated by glutathione (G) and nickel (N) resin. (C) The Mob1 and (D) Mob2 kinase restrictor motif (KRM) interacts with Ndr/Lats^{NTR}. (C) Mob1 containing either the wild-type (1) or Mob2 (2) KRM with Dbf2^{NTR} or Cbk1^{NTR} were co-expressed in BL21(DE3) and purified. Lane 1, Dbf2^{NTR} –Mob1^{WT}; 2, Dbf2

^{NTR} -Mob1 ^{Mob2KRM}; 3, Cbk1 ^{NTR} -Mob1 ^{WT}; 4, Cbk1 ^{NTR} –Mob1^{Mob2KRM}. (D) Mob2 containing the Mob1 (1) or Mob2 (2) KRMs co-expressed with Dbf2 ^{NTR} or Cbk1 ^{NTR} similarly. Lane 1, Dbf2 ^{NTR} -Mob2 ^{WT}; 2, Dbf2 ^{NTR} -Mob2 ^{Mob1KRM}; 3, Cbk1 ^{NTR} -Mob2 ^{WT}; 4, Cbk1 ^{NTR} -Mob2 ^{Mob1KRM}. Lane 5 in all cases is a control with either Mob1 ^{Mob2KRM} or Mob2 ^{Mob1KRM}. The cartoon (bottom) describes the experiment; Mob1, dark red; Mob2, orange. Mutants: Mob1 ^{Mob2KRM}, Mob1$^{R149K\ G150Y\ E151V}$; Mob2 ^{Mob1KRM}, Mob2$^{K118R\ Y119G\ V128E}$. (*) Denotes degradation products of the NTR.

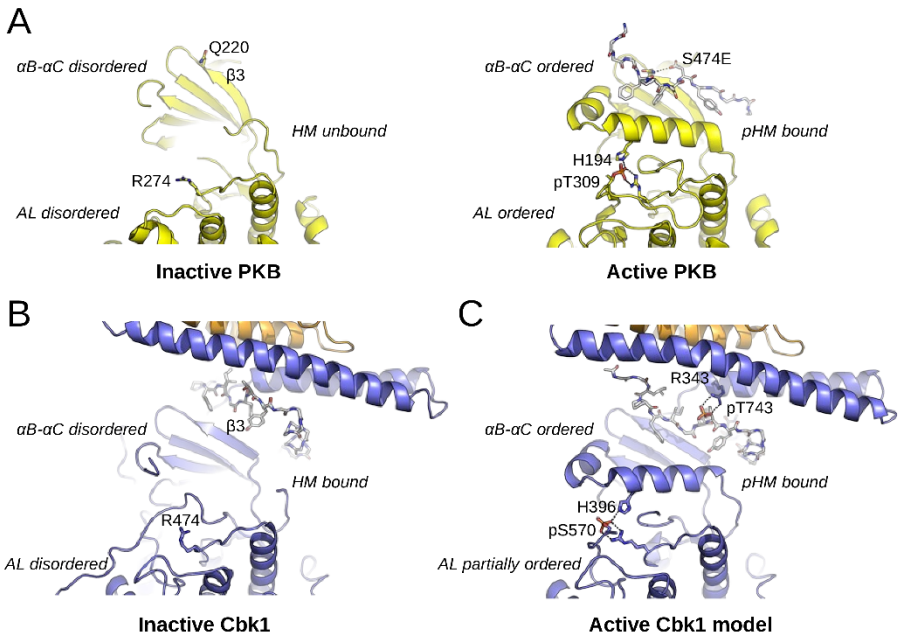

Figure 6 Cbk1 activation: the role of HM phosphorylation and Mob binding

(A) The activation of PKB involves a disorder-to-order transition at the αB-αC segment, the activation loop (AL) and the HM. (B) The inactive Cbk1 structure shows a similar structure apart from the position of its HM. The inactive crystal structure of the Cbk1-Mob2 shows that the HM is bound to the groove formed by the Mob bound NTR and β3 from Cbk1. (C) For activation, the ordering of αC helix in Cbk1

similarly to PKB is likely required (MD model). This latter may be supported by interactions formed by phospho-HM and phospho-AL. The activation loop phosphosite (PKB: Thr-309, Cbk1: Ser-570) is coordinated by an arginine residue from the kinase HRD motif (PKB: Arg-274, Cbk1: Arg-474) and by another residue from the αC helix (PKB: His-194, Cbk1: His-396). The hydrophobic motif phosphosite (PKB: Ser-474, Cbk1: Thr-743) in most AGC kinases is coordinated by a single residue from β3 (PKB: Gln-220). In the case of Cbk1 an arginine residue (Arg-343) from the Mob bound αMobB coordinates the HM phosphosite while β3 may not be involved. Both for PKB and Cbk1 phospho-HM coordination (by Gln-220-pSer-474 or by Arg-343-pThr-743) bring hydrophobic residues much closer to the αC and probably facilitates its ordering. This activation model suggests that co-activator binding is not only essential in HM binding but also in the precise coordination of the kinase's active state when it is phosphorylated. PKB is colored in yellow and both HM regions are shown with gray sticks.

Table 1. Crystallographic data collection and refinement

	Dbf2^{NTR}- Mob1	Cbk1^{NTR}- Mob2	Cbk1- Mob2 - pepSsd1
Data collection			
Wavelength (Å)	0.978560	0.978720	1.0000
Space group	P 6_1 2 2	P 4_1 2_1 2	C 1 2 1
Cell dimensions			
a, *b*, *c* (Å)	108.28,108.28, 134.76	126.23, 126.27, 49.34	138.43, 79.99, 117.59
α, β, γ (°)	90.0, 90.0, 120.0	90.0, 90.0, 90.0	90.0, 117.6, 90.0
Resolution (Å)	46.9-3.5 (3.59-3.50)	39.9-2.8 (2.87-2.80)	44.60-3.15 (3.23-3.15)
$CC_{1/2}$	99.0 (79.1)	100.0 (67.0)	99.6 (80.4)
R_{merge}	54.1 (259.2)	10.0 (152.4)	16.8 (130.4)
Mean $I/\sigma I$	9.34 (1.49)	21.79 (2.21)	9.37 (2.05)
Completeness (%)	99.9 (100)	99.8 (100)	99.7 (99.7)
Redundancy	24.60 (25.83)	14.16 (14.74)	7.73 (7.82)
No. reflections	6385 (447)	10323 (750)	19888 (1455)
Refinement			
R_{work}/ R_{free}	0.2292/0.2631	0.2490/0.2838	0.2310/0.2983
No. atoms			
Protein	2024	2196	4715
Ligand/ion	17	1	31
B-factors			
Protein	88.3	92.7	98.8
Ligand	139.1	114.7	92.6
Ramachandran			
Favored (%)	93.5	93	76**
Allowed (%)	5	4	23**
Outliers (%)	1.6	3	1**
Rotamer outliers (%)	1.85	15	21.5
R.m.s deviations			
Bond lengths (Å)	0.010	0.004	0.011
Bond angles (º)	0.75	0.70	1.35

*Highest resolution shell is shown in parenthesis.

**Ramachandran restraints were used during refinement.